 CMES, vol.51, no.3, pp.261-276, 2009

A Fictitious Time Integration Method for Backward Advection-Dispersion Equation

Chih-Wen Chang[1] **and Chein-Shan Liu**[2]

Abstract: The backward advection-dispersion equation (ADE) for identifying the groundwater pollution source identification problems (GPSIPs) is numerically solved by employing a fictitious time integration method (FTIM). The backward ADE is renowned as ill-posed because the solution does not continuously count on the data. We transform the original parabolic equation into another parabolic type evolution equation by introducing a fictitious time coordinate, and adding a viscous damping coefficient to enhance the stability of numerical integration of the discretized equations by employing a group preserving scheme. When several numerical examples are amenable, we find that the FTIM is applicable to retrieve all past data very well and is good enough to deal with heterogeneous parameters. Even under seriously noisy final data, the FTIM is also robust against disturbance.

Keywords: Groundwater contaminant distribution, Advection-dispersion equation, Inverse problem, Fictitious time integration method (FTIM), Group preserving scheme (GPS)

1 Introduction

Over the past decades, a number of studies have been done to cope with the backward advection-dispersion equation (ADE) for identifying the groundwater pollution source identification problem (GPSIP). One often uses an optimization method to attain the best fitted solution owing to the easy implement of numerical procedures. Gorelick et al. (1983) first formulated the problem as a forward simulation in conjunction with a linear optimization model by employing the multiple regression and linear programming. The optimization model offers an effective method to identifying the location and time release history of groundwater pollution source

[1] Grid Application Division, National Center for High-Performance Computing, Taichung 40763, Taiwan

[2] Department of Civil Engineering, National Taiwan University, Taipei 10617, Taiwan. Corresponding author, E-mail address: liucs@ntu.edu.tw

in homogeneous medium. Nevertheless, the classical optimization approach takes much computational time, produces large numerical errors, and is confined to cases where the data are available in the form of breakthrough curves. Since the GPSIP is a nonlinear problem, Wagner (1992) has proposed a combination of the nonlinear optimization model and the nonlinear maximum likelihood estimation to deal with the parameter estimations and groundwater contaminant source characterizations in the homogeneous medium simultaneously; and reported that the nonlinear optimization method is more accurate than the linear optimization approach for solving the location of a pollution source and the reconstruction of the release history because the model parameter uncertainty is considered. However, the nonlinear maximum likelihood estimation has so many constraints that its application is limited, and its complicated procedures need to be tackled. In general, the above-mentioned optimization methods encounter complicated procedures and large numerical errors in coping with the problem in heterogeneous media.

To resolve the GPSIP in heterogeneous media, Atmadja (2001) and Atmadja and Bagtzoglou (2001a, 2001b, 2003) have proposed the marching-jury backward beam equation (MJBBE) method, which dealt with the recovery of the spatial distribution of contaminant concentration and was not an optimization method. Calculating from the recovery of the spatial distribution of contaminant concentration in homogeneous media, the MJBBE method yields smaller numerical errors than those in heterogeneous media (see Fig. 5 and Figs. 8-11 of Atmadja and Bagtzoglou (2001b)). However, the approach recovers the problem only in a short time period between the initial and final time, and it transforms the second-order backward ADE into the fourth-order PDE. This transform not only increases the complexity of the computational procedures, where two artificial boundary conditions are required, and also spends much computational time. Besides, the numerical errors of the MJBBE method are larger than those calculated by the forward numerical approach. After that, Wang and Zabaras (2006) employed a hierarchical Bayesian computational method to solve the one-dimensional backward ADE. However, the computational procedures of their approach are complicated, and their method needs many iterations. Subsequent to Wang and Zabaras (2006), Liu et al. (2010) employed the backward group preserving scheme (BGPS) to solve the backward ADE. This paper shows that the recovery time of the plume spatial distribution of the BGPS is longer than that of the MJBBE method. Especially, the one-step BGPS has some merits than other numerical methods due to its group structure and no error propagation in the one-step computation.

In this paper, we propose the fictitious time integration method (FTIM) for solving the GPSIP. The FTIM is first proposed by Liu and Atluri (2008a), in which the large scale nonlinear algebraic equations are solved. Later, the FTIM is used to tackle the

mixed complementarity problems with applications to nonlinear optimization [Liu and Atluri (2008b)], to resolve the discretized inverse Sturm-Liouville problems [Liu and Atluri (2008c)], to solve the two-dimensional quasilinear elliptic boundary value problems [Liu (2008a)], to deal with the non-linear obstacle problems with the aid of an NCP-function [Liu (2008b)], to solve the Burgers equation [Liu (2009a)], to cope with the m-point boundary value problem [Liu (2009b)], and to treat the Fredholm integral equation of the first-kind and perform numerical differentiation of noisy data [Liu and Atluri (2009)]. Lately, Ku, Yeih, Liu and Chi (2009) have proposed a new modified time-like function of FTIM to accelerate the numerical convergence. Among these endeavors, the FTIM has shown its powerful noise resistance for coping with the ill-posed behaviors.

2 Groundwater pollution source identification problem

Let us consider the following one-dimensional backward ADE:

$$\frac{\partial C}{\partial t} = \frac{\partial}{\partial x}\left[D\frac{\partial C}{\partial x}\right] - v\frac{\partial C}{\partial x} \tag{1}$$

$$C(0,\, t) = C(l,\, t) = 0,\ 0 \le t \le T, \tag{2}$$

$$C(x,\, T) = C_T(x),\ 0 \le x \le l, \tag{3}$$

where C is the solute concentration, D is a constant dispersion coefficient, v is the transport velocity in the x direction, and $C_T(x)$ is the observed plume's spatial distribution at a time T. The domain is assumed to be sufficiently large that the plume has not reached the boundary.

3 Solving backward ADE by FTIM

3.1 Transformation into a different evolutional PDE and semi-discretization of ADE

First, we propose the following transformation:

$$E(x,\, t, \tau) = (1+\tau)C(x,\, t), \tag{4}$$

and introduce a viscosity damping coefficient ν in Eq. (1):

$$0 = -\nu\frac{\partial C}{\partial t} + \nu D\frac{\partial^2 C}{\partial x^2} - v\nu\frac{\partial C}{\partial x}. \tag{5}$$

Multiplying the above equation by $1 + \tau$ and employing Eq. (4), we have

$$0 = -\nu\frac{\partial E}{\partial t} + \nu D\frac{\partial^2 E}{\partial x^2} - v\nu\frac{\partial E}{\partial x}. \tag{6}$$

Recalling that $\partial E/\partial \tau = C(x,t)$ by Eq. (4), and adding it on both the sides of the above equation we obtain

$$\frac{\partial E}{\partial \tau} = -v\frac{\partial E}{\partial t} + vD\frac{\partial^2 E}{\partial x^2} - vv\frac{\partial E}{\partial x} + C. \tag{7}$$

Finally by employing $C = E/(1+\tau)$, we can change Eqs. (1)-(3) into another parabolic type PDE:

$$\frac{\partial E}{\partial \tau} = -v\frac{\partial E}{\partial t} + vD\frac{\partial^2 E}{\partial x^2} - vv\frac{\partial E}{\partial x} + \frac{E}{1+\tau}, \tag{8}$$

$$E(0,t,\tau) = E(l,t,\tau) = 0,\ 0 \le t \le T, \tag{9}$$

$$E(x,T,\tau) = (1+\tau)C_T(x),\ 0 \le x \le l\ . \tag{10}$$

There is maybe another selection of Eq. (4) by employing $E = p(\tau)C$, where we require that $p(0) = 1$. When $p(\tau)$ is more complicated than 1 + τ the resulting PDE is more complex than Eq. (8). However, other choices are possible if they can supply a better result than the present one.

Applying a semi-discrete procedure to Eq. (8) yields a coupled system of ordinary differential equations (ODEs):

$$\dot{E}_{i,l} = \frac{-v}{\Delta t}\left[E_{i,l+1} - E_{i,l}\right] + \frac{vD}{(\Delta x)^2}\left[E_{i+1,l} - 2E_{i,l} + E_{i-1,l}\right] - \frac{vv}{2\Delta x}\left[E_{i+1,l} - E_{i-1,l}\right] + \frac{E_{i,l}}{1+\tau}, \tag{11}$$

where Δx is a uniform spatial length in the x direction, Δt is a time stepsize, $E_{i,l}(\tau) = E(x_i,\ t_l, \tau)$, and $\dot{E}$ denotes the differential of E with respect to τ.

When one employs a suitable numerical integrator to integrate Eq. (11), a sequence of $E_{i,l}$ can be obtained. Given a stopping criterion, as shown below, to terminate the fictitious time stepping solution, we can obtain the solution of E at a fictitious time τ_f, and calculating C by Eq. (4), we can attain the solution of C in a fully spacetime region. Therefore, we call this novel approach a fictitious time integration method (FTIM).

3.2 GPS for differential equations system

We can write Eq. (11) as a vector form:

$$\dot{\mathbf{E}} = \mathbf{f}(\mathbf{E}, \tau),\ \mathbf{E} \in R^n,\ \tau \in R, \tag{12}$$

where $\mathbf{E}$ is an n-dimensional state vector, and $\mathbf{f} \in R^n$ is a vector-valued function of $\mathbf{E}$ and τ.

The GPS can preserve the internal symmetry group of the considered ODE system. For nonlinear differential equations systems, Liu (2001) has embedded them into the augmented dynamical systems, which concern with not only the evolution of state variables but also the evolution of the magnitude of state variables vector.

We can embed Eq. (12) into the following $n+1$-dimensional augmented dynamical system:

$$\frac{d}{d\tau}\begin{bmatrix}\mathbf{E}\\ \|\mathbf{E}\|\end{bmatrix} = \begin{bmatrix}0_{n\times n} & \frac{\mathbf{f}(\mathbf{E},\tau)}{\|\mathbf{E}\|}\\ \frac{\mathbf{f}^T(\mathbf{E},\tau)}{\|\mathbf{E}\|} & 0\end{bmatrix}\begin{bmatrix}\mathbf{E}\\ \|\mathbf{E}\|\end{bmatrix}. \tag{13}$$

Here, we assume $\|\mathbf{E}\| > 0$ and hence, the above system is well-defined.

It is obvious that the first row in Eq. (13) is the same as the original Eq. (12), but the inclusion of the second row in Eq. (13) gives us a Minkowskian structure of the augmented state variables of $\mathbf{X} := (\mathbf{E}^T, \|\mathbf{E}\|)^T$, which satisfies the cone condition:

$$\mathbf{X}^T\mathbf{g}\mathbf{X} = 0, \tag{14}$$

where

$$\mathbf{g} = \begin{bmatrix}\mathbf{I}_n & 0_{n\times 1}\\ 0_{1\times n} & -1\end{bmatrix} \tag{15}$$

is a Minkowski metric. $\mathbf{I}_n$ is the identity matrix of order n, and the superscript T denotes the transpose. In terms of $(\mathbf{E}^T, \|\mathbf{E}\|)$, Eq. (14) holds, as

$$\mathbf{X}^T\mathbf{g}\mathbf{X} = \mathbf{E}\cdot\mathbf{E} - \|\mathbf{E}\|^2 = \|\mathbf{E}\|^2 - \|\mathbf{E}\|^2 = 0, \tag{16}$$

where the dot between two n-dimensional vectors represents their Euclidean inner product. The cone condition is thus the most natural constraint that we can impose on the dynamical system (13).

Consequently, we have an $n+1$-dimensional augmented system:

$$\dot{\mathbf{X}} = \mathbf{A}\mathbf{X} \tag{17}$$

with a constraint (14), where

$$\mathbf{A} := \begin{bmatrix}0_{n\times n} & \frac{\mathbf{f}(\mathbf{E},\tau)}{\|\mathbf{E}\|}\\ \frac{\mathbf{f}^T(\mathbf{E},\tau)}{\|\mathbf{E}\|} & 0\end{bmatrix} \tag{18}$$

is an element of the Lie algebra $so(n,1)$ of the proper orthochronous Lorentz group $SO_o(n,1)$, satisfying

$$\mathbf{A}^T\mathbf{g}+\mathbf{g}\mathbf{A}=0. \tag{19}$$

This fact prompts us to employ the group preserving scheme (GPS), and its discretized mapping $\mathbf{G}$ exactly preserves the following properties:

$$\mathbf{G}^T\mathbf{g}\mathbf{G}=\mathbf{g}, \tag{20}$$

$$\det\mathbf{G}\ =1, \tag{21}$$

$$G_0^0>0, \tag{22}$$

where G_0^0 is the 00th component of $\mathbf{G}$. Such $\mathbf{G}$ is an element of $SO_o(n,1)$. The term orthochronous should be understood as the preservation of the sign of $\|\mathbf{E}\|>0$.

Although the dimension of the new system rises by one, it has been shown that the new system has the advantage of admitting a GPS given as follows [Liu (2001)]:

$$\mathbf{X}_{l+1}=\mathbf{G}(l)\mathbf{X}_l, \tag{23}$$

where $\mathbf{X}_l$ stands for the numerical evaluation of $\mathbf{X}$ at the discrete time τ_l, and $\mathbf{G}(l)\in SO_o(n,1)$ is the group evaluation at time τ_l.

To give a step by step numerical scheme, we suppose that $\mathbf{A}(l)$ in Eq. (17) is a constant matrix, taking its value at the l-th step. An exponential mapping of $\mathbf{A}(l)$ for the interval $\tau_l\le\tau<\tau_l+\Delta\tau$, when the time parameter τ in Eq. (18) is approximately fixed as $\tau=\tau_l$, admits:

$$\mathbf{G}(l)=exp[\Delta\tau\mathbf{A}(l)]=\begin{bmatrix}\mathbf{I}_n+\frac{(a_l-1)}{\|\mathbf{f}_l\|^2}\mathbf{f}_l\mathbf{f}_l^T & \frac{b_l\mathbf{f}_l}{\|\mathbf{f}_l\|}\\ \frac{b_l\mathbf{f}_l^T}{\|\mathbf{f}_l\|} & a_l\end{bmatrix}, \tag{24}$$

where

$$a_l:=\cosh\left(\frac{\Delta\tau\,\|\mathbf{f}_l\|}{\|\mathbf{E}_l\|}\right),\ b_l:=\sinh\left(\frac{\Delta\tau\,\|\mathbf{f}_l\|}{\|\mathbf{E}_l\|}\right). \tag{25}$$

For saving notation, we use $\mathbf{f}_l=\mathbf{f}(\mathbf{E}_l,\ \tau_l)$. Substituting Eq. (24) for $\mathbf{G}(l)$ into Eq. (23) and taking its first row, we obtain

$$\mathbf{E}_{l+1}=\mathbf{E}_l+\frac{(a_l-1)\mathbf{f}_l\cdot\mathbf{E}_l+b_l\,\|\mathbf{E}_l\|\ \ \|\mathbf{f}_l\|}{\|\mathbf{f}_l\|^2}\mathbf{f}_l=\mathbf{E}_l+\eta_l\mathbf{f}_l, \tag{26}$$

where η_l is an adaptive factor. From $\mathbf{f}_l \cdot \mathbf{E}_l \geq -\|\mathbf{f}_l\| \ \|\mathbf{E}_l\|$, we can prove that

$$\eta_l \geq \left[1 - \exp\left(-\frac{\Delta\tau\,\|\mathbf{f}_l\|}{\|\mathbf{E}_l\|}\right)\right] \frac{\|\mathbf{E}_l\|}{\|\mathbf{f}_l\|} > 0, \ \forall \Delta\tau > 0. \tag{27}$$

This scheme is group properties preserved for all $\Delta\tau > 0$, and is called the group preserving scheme.

3.3 The convergent criterion

We use the above GPS to integrate Eq. (11) from $\tau = 0$ to a selected fictitious final time τ_f. In the numerical integration process, we can examine the convergence of $E_{i,l}$ at the q- and $q+1$-steps by

$$\sqrt{\sum_{l=1}^{m_1} \sum_{i=1}^{m} [E_{i,l}^{q+1} - E_{i,l}^{q}]^2} \leq \varepsilon, \tag{28}$$

where ε is a selected criterion, m_1 is the number of subintervals in time direction, and m is the number of grid points in spatial direction, presuming the same. If at a time $\tau_0 \leq \tau_f$ the above criterion is satisfied, then the solution of C is given by

$$C_{i,l} = \frac{E_{i,l}(\tau_0)}{1+\tau_0}. \tag{29}$$

Practically, if a suitable τ_f is selected, we discover that the numerical solution also approaches the true solution very well, even the above convergent criterion is not satisfied. The coefficient ν introduced in Eq. (11) can increase the stability of numerical integration.

Particularly, we would stress that the present approach is a new FTIM, which can calculate the parabolic PDE very effectively and stably. In Section 4, we give several numerical examples to show some merits of the proposed FTIM.

4 Numerical examples

We will apply the FTIM to the calculation of backward ADE through numerical examples. We are interested in the stability of our approach when the input final measured data are polluted by random noise. We can evaluate the stability by increasing the levels of random noise in the final data:

$$\hat{C}_T = C_T + sR(i), \tag{30}$$

where C_T is the exact data. We use the function RANDOM_NUMBER given in Fortran to generate the noisy data $R(i)$, which are random numbers in (0, 1), and

s means the level of absolute noise. Then, the noisy data $\hat{C}_T$ are employed in the calculations. Usually, when the exact data is small, we use relative random noise to represent noise

$$s_r = \frac{s}{|C_T^{max}|} \times 100\%, \tag{31}$$

where C_T^{max} is the maximum data.

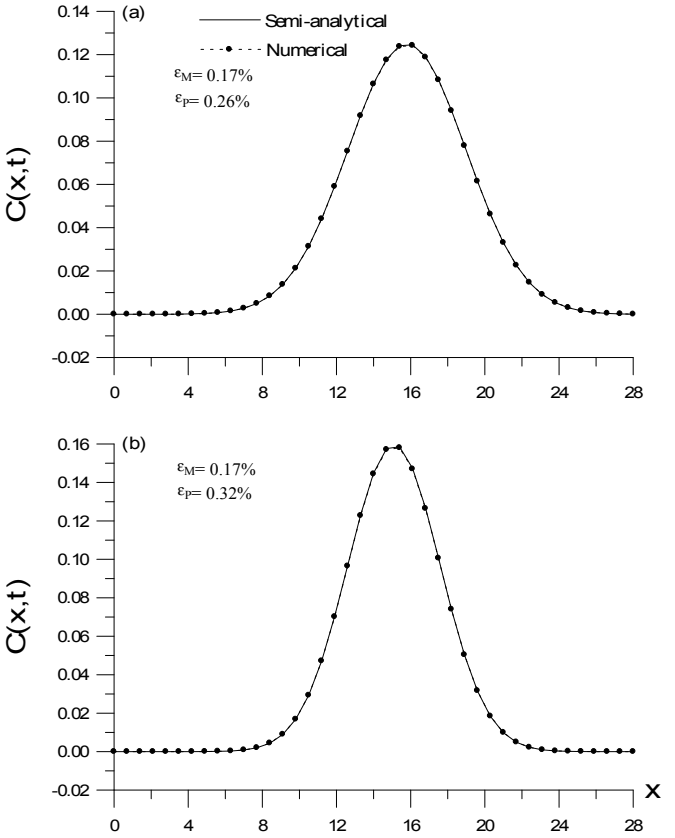

Figure 1: Comparisons of semi-analytical solutions and numerical solutions for homogeneous ADE problem with data at different times been retrieved: (a) t = 1.8, (b) t = 1.1.

4.1 FTIM for the homogeneous ADE

Under the following parameters: m = 40, m_1 = 40, $\varepsilon = 10^{-3}$, $\nu = 10^{-4}$, t = 1.8, D = 2.8, v = 1, l = 28, and a fictitious terminal time τ_f = 39, and starting from an

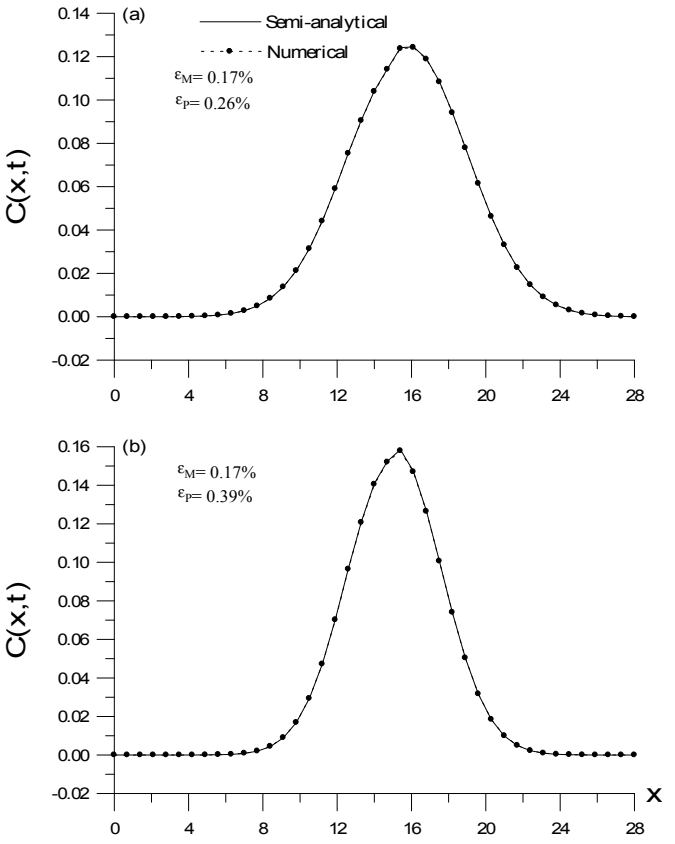

Figure 2: Comparisons of semi-analytical solutions and numerical solutions for configuration 1 with data at different times been retrieved: (a) t = 1.8, (b) t = 1.1.

initial value of $E_{i,l} = 0.95 \sum_{k=1}^{100} a_k e^{vx_i/2D} \sin \frac{k\pi x_i}{l}$, we solve this problem by the present approach with a fictitious time stepsize $\Delta\tau = 0.1$. In Fig. 1, we show the numerical results and the errors for a final time of $T = 2$. Two cases in Figs. 1(a) for $t = 1.8$ and 1(b) for $t = 1.1$ are obtained by FTIM. Upon compared with the numerical results computed by Atmadja and Bagtzoglou (2001) with the MJBBE (see Fig. 5 of the above cited paper) and Wang and Zabaras (2006) with a hierarchical Bayesian computation method, we can say that the FTIM is more accurate than the MJBBE for this example. The output data are also summarized in Table 1.

From Table 2, we reveal that the accuracy in the mass errors and the peak errors are slightly different for $\Delta x = 28/28$, 28/40, 28/75, 28/100, and 28/115, and the

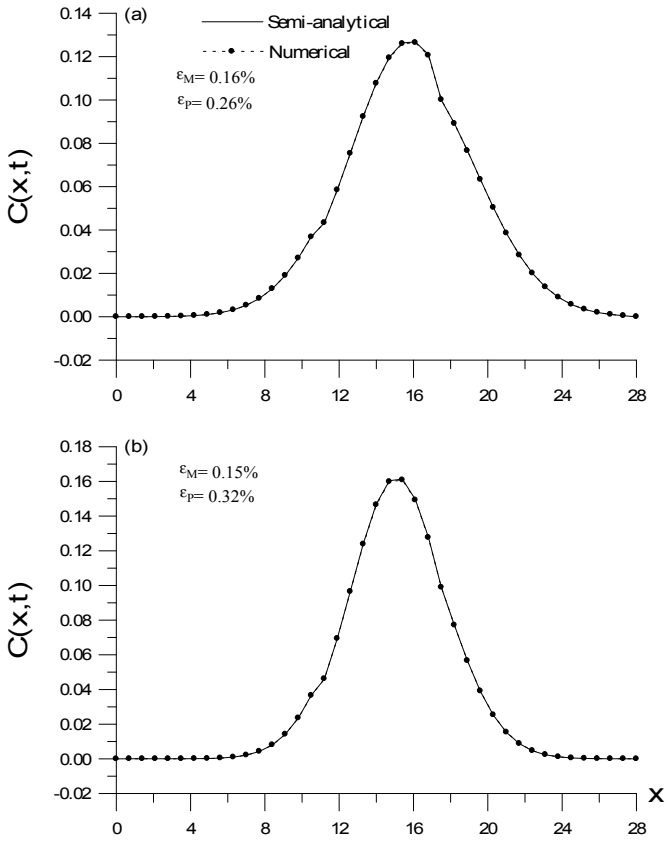

Figure 3: Comparisons of semi-analytical solutions and numerical solutions for configuration 2 with data at different times been retrieved: (a) t = 1.8, (b) t = 1.1.

Table 1: Comparing the mass and concentration peak errors of FTIM and MJBBE of homogeneous ADE problem.

	$\varepsilon_M(\%)$		$\varepsilon_P(\%)$	
Time	MJBBE	FTIM	MJBBE	FTIM
$T = 2$ $t = 1.8$	-0.024	0.17	0.41	0.26
$T = 3$ $t = 1.8$		0.17		0.26
$T = 4$ $t = 1.8$		0.17		0.26
$T = 5$ $t = 1.8$		0.17		0.26
$T = 2$ $t = 1.1$	-0.11	0.17	2.61	0.32

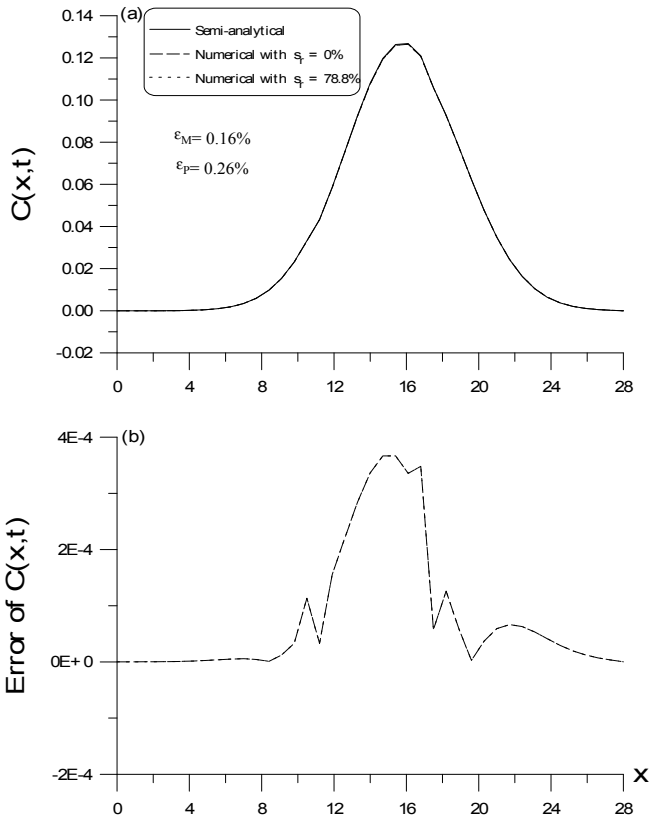

Figure 4: Comparisons of semi-analytical solutions and numerical solutions for configuration 3 with data at $t = 1.8$ retrieved and made in (a) with different noise levels $s_r = 0, 78.8\%$, and (b) the corresponding numerical errors.

Table 2: Summary of mass and concentration peak errors of FTIM of homogeneous ADE problem for different Δx when $\Delta\tau = 0.1$.

	$\varepsilon_M(\%)$		$\varepsilon_P(\%)$	
Δx	$T = 2\ t = 1.8$	$T = 2\ t = 1.1$	$T = 2\ t = 1.8$	$T = 2\ t = 1.1$
$\frac{28}{28}$	0.17	0.17	0.26	0.34
$\frac{28}{50}$	0.17	0.17	0.28	0.34
$\frac{28}{75}$	0.17	0.17	0.28	0.35
$\frac{28}{100}$	0.17	0.17	0.28	0.34
$\frac{28}{115}$	0.17	0.17	0.27	0.34

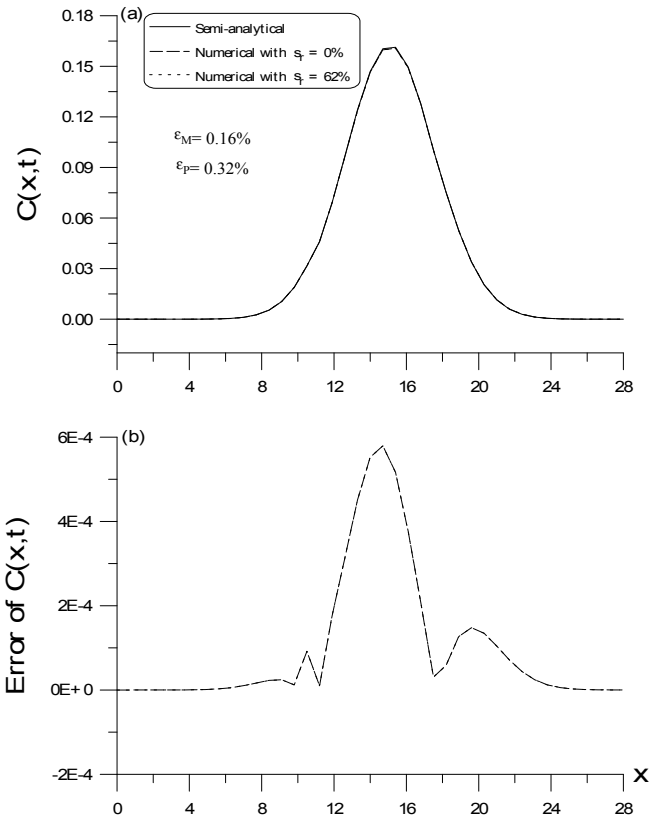

Figure 5: Comparisons of semi-analytical solutions and numerical solutions for configuration 3 with data at t = 1.1 retrieved and made in (a) with different noise levels s_r = 0, 62%, and (b) the corresponding numerical errors.

Table 3: Summary of mass and concentration peak errors of FTIM of homogeneous ADE problem for different $\Delta\tau$ when $\Delta x = 28/40$.

	$T = 2\ t = 1.8$			$T = 2\ t = 1.1$	
$\Delta\tau$	$\varepsilon_M(\%)$	$\varepsilon_P(\%)$	$\Delta\tau$	$\varepsilon_M(\%)$	$\varepsilon_P(\%)$
0.15	-2.46	-2.31	0.15	-2.46	-2.23
0.1	0.17	0.26	0.1	0.17	0.32
0.05	2.69	2.73	0.05	2.69	2.76

difference in the peak errors is almost negligible. However, reducing $\Delta\tau$ increases the accuracy of the peak errors. For example, from the numerical results at t = 1.1

Table 4: Dispersion coefficient configurations for heterogeneous ADE.

Configuration	D_O	D_i	Inner zone width
1	2.8	3.0	2
2	3.5	2.7	6
3	3.0	2.7	6

we observed that the peak error is decreased from -2.23% for $\Delta\tau = 0.15$ to 0.32% for $\Delta\tau = 0.1$ in Table 3. Nevertheless, decreasing it further to $\Delta\tau = 0.05$ did not increase the FTIM performance.

4.2 FTIM for the heterogeneous ADE

Three cases involving heterogeneity in the dispersion coefficient D are analyzed. In all the heterogeneous parameter cases, the velocity is fixed to one. The heterogeneity configurations are shown in Table 4. Under the following parameters: m = 40, m_1 = 40, $\varepsilon = 10^{-3}$, $\nu = 10^{-4}$, t = 1.8, D_O = 2.8, D_i = 3.0, v = 1, T = 2 and a fictitious terminal time τ_f = 39, and starting from an initial value of $E_{i,l} = 0.95 \sum_{k=1}^{100} a_k e^{vx_i/2D} \sin \frac{k\pi x_i}{l}$, we solve this problem by our approach with a fictitious time stepsize $\Delta\tau$ = 0.1. Two different zones, each with a distinct value of D, are used. For configuration 1 the two zones are (1) outer zones for $0 \leq x < 13$ and $15 < x \leq 28$, and (2) inner zone for $13 < x \leq 15$. In both configurations 2 and 3, we use (1) outer zones for $0 \leq x < 11$ and $17 < x \leq 28$, and (2) inner zone for $11 < x \leq 17$. The results in Figs. 2(a) and 2(b) are calculated by the FTIM, and keep $\Delta x = 28/40$. Besides, the results in Fig. 3 are calculated by the FTIM with D_O = 3.5 and D_i = 2.7.

Table 5: Summary of mass and concentration peak errors of FTIM and MJBBE for the heterogeneous ADE cases.

		$\varepsilon_M(\%)$		$\varepsilon_P(\%)$	
Configuration	Time	MJBBE	FTIM	MJBBE	FTIM
1	$T = 2\ t = 1.8$	-0.24	0.17	-0.21	0.26
	$T = 2\ t = 1.1$	-1.10	0.17	-0.87	0.39
2	$T = 2\ t = 1.8$	1.47	0.16	1.78	0.26
	$T = 2\ t = 1.1$	6.79	0.15	8.54	0.32
3	$T = 2\ t = 1.8$	0.63	0.16	0.83	0.26
	$T = 2\ t = 1.1$	2.82	0.16	4.08	0.32

In configuration 3, when the input final measured data are contaminated by random noise, we are concerned about the stability of our method, which is investigated by adding the relative random noise on the final data. The numerical results with $T = 2$ were compared with those without considering random noise in Figs. 4 and 5. Note that when the relative random noises are $s_r = 78.8\%$ and 62%, they disturb the numerical solutions deviating from the semi-analytical solution very small. Upon comparing with the numerical results computed by Atmadja and Bagtzoglou (2001) with the MJBBE (see Figs. 8, 10 and 11 of the above cited paper), we can say that the FTIM is much more accurate than the MJBBE for these examples. The mass errors of Figs. 1 to 3 induced by the FTIM for heterogeneous and homogeneous cases at $t = 1.8$ are small. A summary of the mass and peak errors for different heterogeneity configurations can be found in Table 5. It can been seen that for those examples our results are much better than those obtained by Atmadja and Bagtzoglou (2001). The numerical results with $T = 2$ were compared with those without considering random noise in Figs. 4 and 5. Note that the relative noise level with $s_r = 78.8\%$ and 62%, respectively, disturb the numerical solutions deviating from the semi-analytical solutions small.

5 Conclusions

In this paper, we have transformed the original parabolic equation into another parabolic type evolution equation by introducing a fictitious time coordinate, and adding a viscous damping coefficient to enhance the stability of numerical integration of the discretized equations by using a GPS. Meanwhile, we merely required spending a certain time for integrating the discretized equations. By employing the FTIM we can retrieve the initial data very well with a high order accuracy. Several numerical examples of the GPSIP were worked out, and showed that our proposed approach is applicable to the GPSIP, even for the very severely ill-posed problems. Under the noisy final data, the FTIM is also very robust to recover the initial data. The coefficient ν may be positive or negative dependent on different problems; suitable ν can increase the stability of numerical integration and speeds up the convergence. Therefore, we may conclude that the present FTIM is stable, effective, and accurate. Its numerical implementation is simple and the computation speed is fast.

References

Atmadja, J. (2001): The marching-jury backward beam equation method and its application to backtracking non-reactive plumes in groundwater. Ph.D. Dissertation, Columbia University, New York.

Atmadja, J.; Bagtzoglou, A. C. (2001a): State of the art report on mathematical methods for groundwater pollution source identification. *Environ. Forensics*, vol. 2, pp. 205–214.

Atmadja, J.; Bagtzoglou, A. C. (2001b): Pollution source identification in heterogeneous porous media. *Water Resour. Res.*, vol. 37, pp. 2113–2125.

Atmadja, J.; Bagtzoglou, A. C. (2003): Marching-jury backward beam equation and quasi-reversibility methods for hydrologic inversion: Application to contaminant plume spatial distribution recovery. *Water Resour. Res.*, vol. 39, pp. 1038–1051.

Gorelick, S. M.; Evans, B. E.; Remson, I. (1983): Identifying sources of groundwater pollution: An optimization approach. *Water Resour. Res.*, vol. 19, pp. 779–790.

Ku, C.-Y.; Yeih W.-C.; Liu, C.-S.; Chi, C.-C. (2009): Applications of the fictitious time integration method using a new time-like function. *CMES: Computer Modeling in Engineering & Sciences*, vol. 43, pp. 173–190.

Liu, C.-S. (2001): Cone of non-linear dynamical system and group preserving schemes. *Int. J. Non-Linear Mech.*, vol. 36, pp. 1047–1068.

Liu, C.-S. (2008a): A fictitious time integration method for two-dimensional quasi-linear elliptic boundary value problems. *CMES: Computer Modeling in Engineering & Sciences*, vol. 33, pp.179–198.

Liu, C.-S. (2008b): A time-marching algorithm for solving non-linear obstacle problems with the aid of an NCP-function. *CMC: Computers, Materials & Continua*, vol. 8, pp. 53–66.

Liu, C.-S. (2009a): A fictitious time integration method for the Burgers equation. *CMC: Computers, Materials & Continua*, vol. 9, pp. 229–252.

Liu, C.-S. (2009b): A fictitious time integration method for solving m-point boundary value problems. *CMES: Computer Modeling in Engineering & Sciences*, vol. 39, pp. 125–154.

Liu, C.-S.; Atluri, S. N. (2008a): A novel time integration method for solving a large system of non-linear algebraic equation. *CMES: Computer Modeling in Engineering & Sciences*, vol. 31, pp. 71-83.

Liu, C.-S.; Atluri, S. N. (2008b): A fictitious time integration method (FTIM) for solving mixed complementarity problems with applications to non-linear optimization. *CMES: Computer Modeling in Engineering & Sciences*, vol. 34, pp. 155-178.

Liu, C.-S.; Atluri, S. N. (2008c): A novel fictitious time integration method for solving the discretized inverse Sturm-Liouville problems, for specified eigenvalues.

CMES: Computer Modeling in Engineering & Sciences, vol. 36, pp. 261-286.

Liu, C.-S.; Atluri, S. N. (2009): A fictitious time integration method for the numerical solution of the Fredholm integral equation and for numerical differentiation of noisy data, and its relation to the filter theory. *CMES: Computer Modeling in Engineering & Sciences*, vol. 41, pp. 243-262.

Liu, C.-S.; Chang, C.-W.; Chang, J.-R. (2010): The backward group preserving scheme for 1D backward in time advection-dispersion equation. *Num. Methods Partial Diff. Eqns.*, vol. 26, pp. 61–80.

Wagner, B. J. (1992): Simultaneous parameter estimation and contaminant source characterization for coupled groundwater flow and contaminant transport modeling. *J. Hydrol.*, vol. 135, pp. 275–303.

Wang, J.; Zabaras, N. (2006): A Markov random field model of contamination source identification in porous media flow. *Int. J. Heat Mass Transfer*, vol. 49, pp. 939–950.